COMMUNICATION

Near infrared light-driven liquid crystal phase transition enabled by hydrophobic mesogen grafted plasmonic gold nanorods†

Karla G. Gutierrez-Cuevas,‡[a] Ling Wang,‡[a] Chenming Xue,[a] Gautam Singh,[b] Satyendra Kumar,[b] Augustine Urbas[c] and Quan Li*[a]

Light-driven phase transition in liquid crystals is a fascinating endeavour from both scientific and technological points of view. Here we demonstrate the proof-of-principle that the photothermal effect of organo-soluble plasmonic gold nanorods can introduce the phase transition of thermotropic liquid crystals upon near infrared laser irradiation. Interestingly, the reverse process occurs when the laser is switched off.

Gold nanorods (GNRs) are a promising class of metallic anisotropic nanoparticles, which have been widely investigated in different areas such as nanoscience and nanotechnology, biological and biomedical science, sensing, photonics, and metamaterials.[1] Among the unique properties of GNRs, the fascinating "photothermal effect" resulting from the longitudinal surface plasmon resonance (LSPR) has been recently in the limelight. When GNRs are exposed to the laser light resonant with their surface plasmon oscillation, they can strongly absorb the light and rapidly convert it into heat *via* a series of photophysical processes. Since the longitudinal absorption of GNRs can be tuned to the near infrared (NIR) and even the infrared region, the appealing photothermal effect of GNRs has been utilized in biological and biomedical applications. GNRs can be made organo-soluble and compatible with different organic matrices by the incorporation of different kinds of organic molecules onto their surface such as polymers,[2] chromophores,[3] and mesogens,[4] which confer special properties and enable applications like self-assembly, fluorescence quenching, solubility, and drug delivery among others. The combination of organo-solubility and efficient photothermal effects of GNRs provides the necessary thrust for their

application as "nanoheaters" by dispersing them in different organic media and irradiation using an appropriate light source.

In recent years, dedicated research has focused on the study of photoinduced phase transitions stimulated by UV, visible or NIR light in soft materials by the incorporation of different types of nanoparticles or light-driven molecular additives as dopants. For example, single-walled carbon nanotubes (SWNTs) have been used to photoinduce a phase transition in poly(*N*-isopropyl acrylamide) using 1064 nm NIR laser irradiation.[5] Similarly, thermotropic liquid crystalline phases (*e.g.* nematic, cholesteric, smectic, and blue phases)[6] have been reported to undergo phase transitions upon UV or visible light irradiation with the incorporation of photoswitchable moieties such as azobenzene. Nevertheless, the use of UV or visible radiation implies higher energy that could cause material degradation or poor penetration; therefore the use of NIR light is attractive due to its low energy and deeper penetration. Recently, we have demonstrated the use of upconversion nanoparticles as NIR nanotransducers to tune the self-organized helical superstructures of thermotropic chiral liquid crystals by the *in situ* generation of UV and visible light.[7] However, the use of NIR-light to induce phase transitions in thermotropic liquid crystals remains an unexplored arena. Here we present the synthesis and characterization of hydrophobic mesogenic thiol monolayer-protected GNRs (M_6S-GNRs, Scheme 1). The resulting hybrid GNRs were found to be soluble in organic solvents and displayed the typical transverse and longitudinal surface plasmon resonances (SPRs) of GNRs. The protected GNRs were homogeneously dispersible in a commercially available thermotropic nematic liquid crystal host E7. Interestingly, the resultant liquid crystalline nanocomposites were found to exhibit a nematic–isotropic phase transition upon irradiation using an 808 nm NIR laser, caused by the photothermal effect of the plasmonic M_6S-GNRs. To the best of our knowledge, study of such phase transitions in thermotropic liquid crystal nanocomposites has so far not been reported.

The new mesogenic thiol surfactant M_6SH was synthesized in a straightforward manner (see the ESI†). The mesogenic thiol exhibited a wide temperature range of the liquid crystal phase

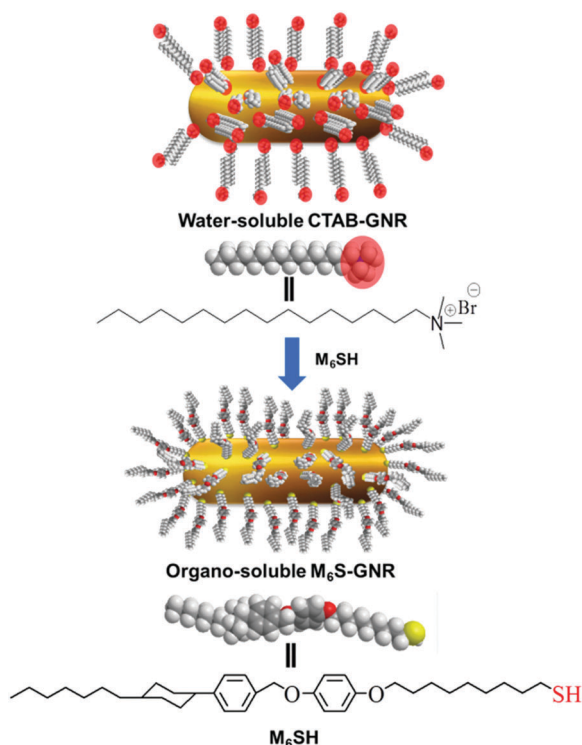[a] *Liquid Crystal Institute, Kent State University, Kent, Ohio, 44242, USA.*
  E-mail: qli1@kent.edu; Tel: +1-330-6721537

[b] *Department of Physics, Kent State University, Kent, Ohio, 44242, USA*

[c] *Materials and Manufacturing Directorate, Air Force Research laboratory WPAFB, Ohio 45433, USA*

Scheme 1 Synthesis of the organo-soluble hybrid M_6S-GNRs by the new hydrophobic mesogenic thiol M_6SH grafted on the GNR *via* the covalent Au–S linkage starting from the as-prepared water-soluble CTAB-GNRs.

as revealed using polarizing optical microscopy (POM) and X-ray diffraction studies (Fig. 1 and ESI†). Upon cooling from the isotropic phase, the mesogenic thiol exhibited a liquid crystal phase from about 116 °C to room temperature. To identify the mesophase structure, we undertook a variable temperature X-ray diffraction study. The sample was heated above the isotropic temperature and cooled down slowly in the presence of an external magnetic field in a 1 mm quartz capillary. In the isotropic phase (120 °C), both small angle and wide angle reflections are diffuse rings as shown in Fig. 1d. These diffuse peaks observed in the isotropic phase change to sharp reflections at
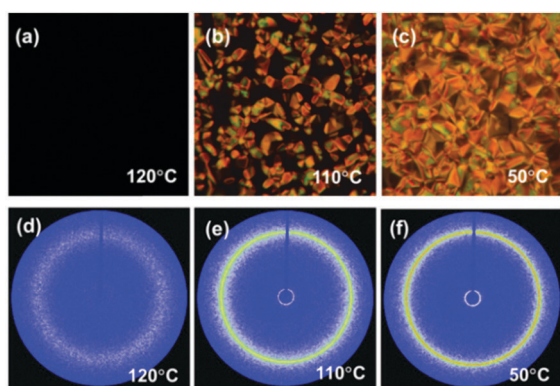
$\sim$115 °C (Fig. S5, ESI†), suggesting the liquid crystal phase to be highly ordered smectic B phase (SmB). Furthermore, lowering the temperature to 50 °C resulted in the same X-ray pattern.

The synthesized liquid crystal thiol M_6SH was reacted with the as-prepared water-soluble cetyltrimethylammonium bromide (CTAB) coated GNRs (CTAB-GNR) through the thiol exchange reaction in order to obtain organo-soluble hybrid M_6S-GNRs. Note that the ionic surfactant CTAB forms a densely packed dynamic surface layer around the side wall of the GNRs which renders them water-soluble, but the CTAB surface layer is dynamically unstable which makes thiol surfactant exchange possible. During the thiol exchange process, the mesogenic thiol monolayer covers the surface of the GNR through strong Au–S covalent linkages. Due to the hydrophobic properties of the mesogenic surfactant, the resulting hybrid M_6S-GNRs were found to be soluble in organic solvents such as chloroform, dichloromethane, and tetrahydrofuran (Fig. S8, ESI†). Both the initial CTAB-GNR and the hybrid M_6S-GNR show two characteristic plasmonic resonance peaks of GNRs (Fig. 2a). No significant broadening of the absorption peaks in the spectrum of the M_6S-GNR compared to the CTAB-GNR suggests the absence of aggregation during the ligand exchange procedure. The mesogenic hybrid M_6S-GNRs were further characterized using TEM (Fig. 2b). The GNRs had an average size of 44.26 ± 3.74 nm $\times$ 14.75 ± 1.75 nm and an aspect ratio of 3.04 ± 0.42 nm based on the calculation of the size of 500 GNRs. The length, width and aspect ratio distribution curves are presented in the ESI,† Fig. S10.

The dispersion quality and compatibility of the mesogen functionalized M_6S-GNRs were explored in the commercially available liquid crystal host E7, which is a eutectic mixture of liquid crystal components designed for display applications and has a wide nematic liquid crystal phase and the nematic–isotropic phase transition (T_{N-I}) around 60 °C. Conventional water-soluble CTAB-GNRs showed poor solubility in E7, leading to phase separation, whereas M_6S-GNRs exhibited good solubility in E7 due to the similarity of the molecular structure of mesogenic thiol M_6SH with the components of E7. The nanocomposites with 0.01%, 0.02%, 0.04%, 0.08%, 0.10%, 0.15%, 0.20%, 0.35% and 0.50 wt% M_6S-GNRs in E7 were investigated using the liquid crystal cells of 25 μm thickness with no alignment layer in order to study their corresponding texture, phase transition temperature as well as the effect of NIR irradiation. The optical textures of their mixtures at 55 °C are shown in the ESI,† Fig. S12, presenting the typical *Schlieren* texture of the nematic liquid crystal. The absence
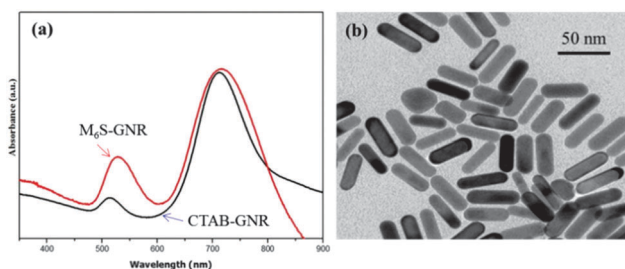

Fig. 1 (a–c) Textures of M_6SH under polarizing optical microscopy at different temperatures in the cell, (a) isotropic phase, (b and c) smectic B phase; (d–f) XRD patterns of M_6SH, (d) isotropic phase, (e and f) smectic B phase.

Fig. 2 (a) UV-visible spectra of CTAB-GNRs in H_2O (black line) and M_6S-GNRs in $CHCl_3$ (red line); (b) the TEM micrograph of M_6S-GNR.

of observable GNR aggregates in the textures indicates that M_6S-GNRs are well dispersed in the liquid crystal matrix. However, if the concentration of M_6S-GNRs is over 0.5 wt%, the resultant liquid crystalline nanocomposite appears inhomogeneous, *i.e.* there is phase separation. Moreover, it was observed that the nematic–isotropic transition temperature of the prepared mixtures was lower than that in pure E7 when the concentration of the M_6S-GNRs reached 0.15 wt% and higher (Table S1, ESI†).

The photothermal effect of the mesogen functionalized M_6S-GNRs to induce the phase transition in the liquid crystalline nanocomposites *via* NIR laser irradiation was investigated. ΔT value was introduced such that $\Delta T = T - T_{I-N}$ where T is the temperature of the liquid crystalline nanocomposite at which the NIR laser irradiation of the sample was performed. This value was used as a standard parameter for each sample because at each concentration of the prepared composites the T_{I-N} differs and decreases when the concentration of nanorods is increased. The irradiation process was performed using an 808 nm NIR laser and the progressive phase transition process was captured using POM. For example, 0.5 wt% M_6S-GNRs in E7 exhibited the typical *Schlieren* texture of the nematic phase (Fig. 3). Upon irradiation using the 808 nm NIR laser for approximately 2 seconds, the liquid crystalline nanocomposites underwent the nematic to isotropic phase transition. Interestingly, the phase transition was found to be reversible when the NIR laser was turned off. The reverse phase transition was observed to occur in approximately 1 second. It is important to note that the pure E7 host did not present a noticeable change under the POM when it was irradiated using the NIR laser under identical conditions. These observations imply that it is the photothermal effect of the embedded GNRs in M_6S-GNRs, resulting in the phase transitions in the nanocomposites. Since the longitudinal surface plasmon resonance of M_6S-GNRs overlaps with the NIR laser frequency, they can absorb the NIR light and convert it into heat (photothermal effect) and convey the thermal energy to the surrounding media, thereby inducing a phase transition. Fig. 4 shows the evolution of the phase transition process for pure E7 and 0.20 wt% M_6S-GNR/E7 with same exposure times at $\Delta T = 4$ °C for comparison. The nanocomposites underwent phase transition in about 7 seconds while the pure E7 mixture did not undergo a phase transition even after 5 minutes.

Furthermore, the time required to change from one phase to another was highly dependent on the concentration of the mesogen coated GNRs. In order to have a better understanding
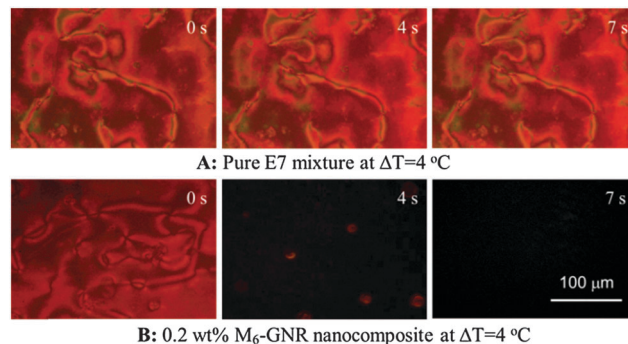

Fig. 4 Photoinduced phase transition of (A) the pure liquid crystal host E7, and (B) the 0.2 wt% M_6-GNR/E7 composite in a 25 μm unaligned cell at $\Delta T = 4$ °C from T_{I-N} at different exposure times.

of the effects of the concentration and temperature on the NIR irradiation process, we systematically monitored different areas in the prepared liquid crystal cells (25 measurements in different regions of the cell), and averaged the response time which is defined as the time taken by the sample to go from the nematic phase to the isotropic state. The time-dependence curve of M_6S-GNR/E7 composites with different concentrations of the M_6S-GNRs is shown in the ESI,† Fig. S13 and S14 at distinct ΔT values. In these experiments, a clear dependence of the phase transition time on the M_6S-GNR concentration is observed and the nanocomposites containing 0.5 wt% M_6S-GNR change rapidly from one phase to the other (0.8 seconds) at $\Delta T = 1$ °C. These results, as anticipated, suggest that the presence of more GNRs contributes to higher efficiency of the photothermal effect in the nanocomposites. It is also evident from the results that when the irradiation is performed further from the T_{I-N}, for example at $\Delta T = 14$ °C, the phase transition process will occur slowly as observed in Fig. S15 (ESI†) while at $\Delta T = 15$ °C, the complete phase change was not observed. For lower concentrations (0.01%) at $\Delta T < 3$ °C, the complete photodriven phase transition was observed at longer exposure times (Fig. S16, ESI†); however, at higher values of ΔT this process was not observed.

In conclusion, the new liquid crystal thiol was synthesized and its liquid crystalline behaviour was characterized *via* the combination of POM and XRD studies. The terminal thiol was grafted onto the surface of the GNR through a strong covalent Au–S linkage. The resultant organo-soluble M_6S-GNRs were incorporated into a commercially available nematic liquid crystal E7 at different concentrations. The homogeneous liquid crystalline nanocomposites were found to undergo a reversible nematic–isotropic phase transition within a few seconds upon NIR laser irradiation, resulting from the photothermal effect of the embedded plasmonic GNRs. The nanocomposites with higher concentration of GNRs exhibited faster phase transitions. The NIR light-induced phase transition demonstrated here might provide impetus in developing new functional stimuli responsive materials where direct heating is not favored.
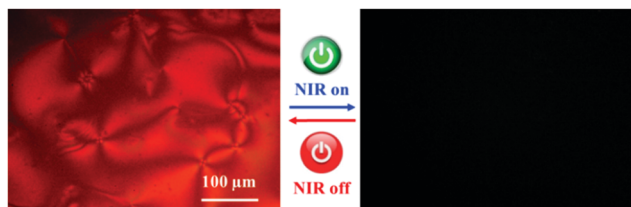
Fig. 3 Phase transition of the 0.5 wt% M_6S-GNR/E7 composite at $\Delta T = 3$ °C with NIR laser irradiation took approximately 2 seconds from the nematic to the isotropic phase whereas it took approximately 1 second to return from the isotropic to the nematic phase when the NIR light was turned off.

Notes and references

1 (a) C. J. Murphy, T. K. Sau, A. M. Gole, C. J. Orendorff, J. X. Gao, L. Gou, S. E. Hunyadi and T. Li, *J. Phys. Chem. B*, 2005, **109**, 13857–13870; (b) C. Xue, O. Birel, M. Gao, S. Zhang, L. Dai, A. Urbas and Q. Li, *J. Phys. Chem. C*, 2012, **116**, 10396–10404.

2 (a) C.-C. Chen, Y.-P. Lin, C.-W. Wang, H.-C. Tzeng, C.-H. Wu, Y.-C. Chen, C.-P. Chen, L.-C. Chen and Y.-C. Wu, *J. Am. Chem. Soc.*, 2006, **128**, 3709–3715; (b) D. Fava, M. A. Winnik and E. Kumacheva, *Chem. Commun.*, 2009, 2571–2573; (c) A. Petukhova, J. Greener, K. Liu, D. Nykypanchuk, R. Nicolaÿ, K. Matyjaszewski and E. Kumacheva, *Small*, 2012, **8**, 731–737.

3 (a) J. M. El Khoury, X. Zhou, L. Qu, L. Dai, A. Urbas and Q. Li, *Chem. Commun.*, 2009, 2109–2111; (b) C. Xue, Y. Xu, Y. Pang, D. Yu, L. Dai, M. Gao, A. Urbas and Q. Li, *Langmuir*, 2012, **28**, 5956–5963; (c) C. Xue, O. Birel, Y. Li, X. Ma, M. Gao, A. Urbas and Q. Li, *J. Colloid Interface Sci.*, 2013, **398**, 1–6.

4 C. Xue, K. Gutierrez-Cuevas, M. Gao, A. Urbas and Q. Li, *J. Phys. Chem. C*, 2013, **117**, 21603–21608.

5 T. Fujigaya and N. Nakashima, in *Single-Walled Carbon Nanotubes as a Molecular Heater for Thermoresponsive Polymer Gel Composite, Chapter 19 in Carbon Nanotubes Polymer Nanocomposites*, ed. S. Yellampalli, InTech, 2011.

6 (a) G. Wang, M. Zhang, Q. Yang, F. Liu, Z. Cheng, R. Guo and H. Yang, *Chem. Lett.*, 2010, **39**, 1144–1145; (b) Q. Li, L. Li, J. Kim, H.-K. Park and J. Williams, *Chem. Mater.*, 2005, **17**, 6018–6021; (c) T.-H. Lin, Y. Li, C.-T. Wang, H.-C. Jau, C.-W. Chen, C.-C. Li, H. K. Bisoyi, T. J. Bunning and Q. Li, *Adv. Mater.*, 2013, **25**, 5050–5054.

7 (a) L. Wang, H. Dong, Y. Li, C. Xue, L.-D. Sun, C.-H. Yan and Q. Li, *J. Am. Chem. Soc.*, 2014, **136**, 4480–4483; (b) L. Wang, H. Dong, Y. Li, R. Liu, Y.-F. Wang, H. K. Bisoyi, L.-D. Sun, C.-H. Yan and Q. Li, *Adv. Mater.*, 2015, **27**, 2065–2069.